



# A neural code for low-frequency sound localization in mammals

David McAlpine<sup>1,2</sup>, Dan Jiang<sup>1</sup> and Alan R. Palmer<sup>1</sup>

<sup>1</sup> MRC Institute of Hearing Research, Science Road, University of Nottingham, Nottingham NG7 2RD, UK

<sup>2</sup> Physiology Department, University College London, Gower Street, London WC1E 6BT, UK

Correspondence should be addressed to D.M. ([d.mcalpine@ucl.ac.uk](mailto:d.mcalpine@ucl.ac.uk))

We report a systematic relationship between sound-frequency tuning and sensitivity to interaural time delays for neurons in the midbrain nucleus of the inferior colliculus; neurons with relatively low best frequencies (BFs) showed response peaks at long delays, whereas neurons with relatively high BFs showed response peaks at short delays. The consequence of this relationship is that the steepest region of the function relating discharge rate to interaural time delay (ITD) fell close to midline for all neurons irrespective of BF. These data provide support for a processing of the output of coincidence detectors subserving low-frequency sound localization in which the location of a sound source is determined by the activity in two broad, hemispheric spatial channels, rather than numerous channels tuned to discrete spatial positions.

For many terrestrial mammals, and particularly for humans, localization of sound sources in the horizontal plane is achieved by an exquisite sensitivity to differences in the fine-time structure of low-frequency (< 1500 Hz) spectral components between the two ears<sup>1–4</sup>. The accepted model to account for this remarkable binaural sensitivity is the coincidence detection model<sup>3</sup>. In this model, an array of neurons receives inputs from the two ears such that a given neuron fires maximally when the difference in arrival time at the two ears resulting from the location of a sound source offsets the difference in neural transmission time. Consistent with this, neurons sensitive to ITDs in the carrier fine structure of low-frequency signals have been recorded from binaurally responsive auditory nuclei in a wide range of species<sup>5–8</sup>. However, the exact means by which ITD-sensitive neurons contribute to localization of a sound source remains to be determined. The prevailing view, explicit in descriptions of localization in the barn owl<sup>9</sup>, and considered to be appropriate for mammals<sup>10</sup>, is that ITD-sensitive neurons signal azimuthal position by their maximal discharge. Each ITD-sensitive neuron can therefore be considered as a separate spatial channel. However, important differences exist between mammalian and barn owl localization abilities and in the mechanisms underlying these abilities. Not the least of these is that barn owls use ITDs to localize high-frequency sounds, in the range 3–9 kHz<sup>9,11,12</sup>, frequencies at which mammals are insensitive to time disparities in the carrier fine structure of the stimulus at the two ears<sup>13</sup>. At these relatively high frequencies, mammalian azimuthal localization is achieved by virtue of differences in the level of the sound between the ears, and complex spectral patterns generated by the frequency-filtering properties of the outer ear<sup>14</sup>. Conversely, barn owls use interaural level differences over this frequency range for localization in the vertical plane<sup>15,16</sup>, combining this with ITD sensitivity in the azimuthal plane to produce a space-specific representation of auditory space in the optic tectum<sup>17</sup>. Furthermore, unlike barn owls<sup>18</sup>, the evidence in mammals for a systematic

arrangement of delay lines feeding the coincidence detectors remains equivocal<sup>19,20</sup>. Little evidence exists that details the distribution of delay sensitivities encoded within the mammalian auditory pathway, and, specifically, it remains unknown how the gradient of axonal delays is arranged across the major tonotopic axis in the medial superior olive (MSO), the site of primary binaural integration in the mammalian brainstem. Finally, electrophysiological data from a single side of the mammalian brainstem and midbrain consistently show the peaks of ITD functions to be distributed around a mean of +200 to +300  $\mu$ s (refs. 5–8), outside the physical limits of many small mammals, and well away from the midline where spatial acuity seems to be greatest<sup>21</sup>. Indeed, the distribution of peak ITDs seems to be an invariant function of head size, with a range of mammalian species demonstrating an almost identical distribution despite large differences in interaural distance<sup>7</sup>. This apparent lack of evolutionary pressure to constrain the peaks of ITD functions to within the physically plausible range is puzzling, and means that for many smaller mammals, most peaks of ITD functions actually fall outside the range they could ever experience. Because acuity tasks, including spatial acuity tasks in other sensory modalities, are normally encoded by over-representation of sensory tissue devoted to the task<sup>22</sup>, it seems incongruous that the peaks of ITD functions should, if anything, be under-represented at interaural delays actually available in the environment.

A tacit assumption in virtually all models of low-frequency binaural hearing is that an identical (and relatively broad) range of peak ITDs is fully represented within each low-frequency channel of the tonotopic gradient, for frequencies up to approximately 2 kHz in mammals<sup>10</sup>. However, no previous study has tested this assumption directly. Here we provide empirical evidence from a large sample of low-BF neurons in the midbrain of the guinea pig, a species with good low-frequency hearing, that mammalian low-frequency localization should be considered in an alternative manner. Our data revealed that the representation of ITDs

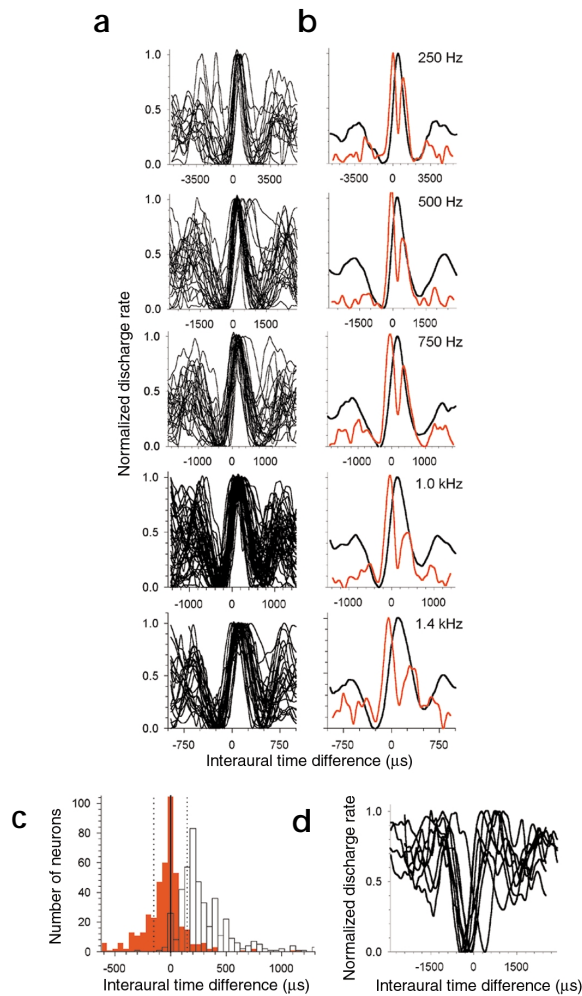


**Fig. 1.** Responses of many ITD-sensitive neurons are maximally modulated over the physiological range of ITDs. **(a)** Noise-delay functions (NDFs) plotting normalized neuronal discharge rate as a function of interaural delay for individual IC neurons over different BF ranges. From top to bottom, NDFs were examined for BFs in a 50-Hz band centered on 250 Hz, 50-Hz bands around 500 Hz and 700 Hz, a 100-Hz band centered on 1.0 kHz, and a 200-Hz band centered on 1.4 kHz. The range over which the ITD functions are plotted is varied so that approximately 2.5 cycles of the BF-dependent oscillatory functions are shown for each BF band. **(b)** Top, NDF for an individual IC neuron with a BF of 250 Hz (black line). Bottom panels, average NDFs (black lines) for the data shown in the left panels of **(a)**. All panels show steepness functions (red lines) for each NDF, in which the absolute slope has been calculated at each ITD. **(c)** Distribution of ITDs at which noise delay functions responded with maximum output (white bars) and at which they responded with maximum change in output (red bars). **(d)** Examples of responses of 'trough-type' neurons, with BFs in the range 450–600 Hz, recorded in the IC. Trough-type neurons were characterized by a minimum discharge rate at a particular value of ITD—often relatively close to zero ITD—and broader regions of higher discharge rate to either side of the trough. Seven of the eight examples here show response minima at ipsilateral ITDs, and one shows a response minimum at a contralateral ITD.

vidual neurons (**Fig. 1b**, black curve in top panel) or averaged across neurons within BF bands (**Fig. 1b**, black curves in remaining panels), NDFs were clearly modulated with the interaural delay of the noise stimulus. Responses tended to peak at positive ITDs, corresponding to sounds that lead in time at the ear contralateral to the IC being recorded. The likely source of binaural input for these IC neurons is the medial superior olive on the same side of the brain<sup>28</sup>. Of the 520 neurons for which we obtained NDFs, most (83%, 432/520) showed peaks at contralaterally leading ITDs (**Fig. 1c**, white bars), consistent with previous reports in the mammalian MSO<sup>29–31</sup> and IC<sup>5–7,32</sup>, and the predominantly ipsilateral projection of the MSO<sup>28</sup>. Most peaks were approximately between +150  $\mu$ s and +300  $\mu$ s, outside the physiological range of the guinea pig. Few neurons showed peaks in their NDFs at or close to zero ITD. A small number of neurons showed NDFs that peaked at negative ITDs (31/520), and about 10% (57/520) showed responses to interaurally delayed noise that were best characterized by a reduction in their response at a particular ITD. Such 'trough-type' neurons (**Fig. 1d**) likely constituted the output of low-frequency neurons in the lateral superior olive (D.J. Tollin, P.X. Joris & T.C.T. Yin, *Abstr. 23rd Meeting Assoc. Res. Otolaryngol.*, 32, 2000).

The representation of ITD in the auditory pathway varied along the tonotopic gradient, that is, with the neuronal BF. The mean (**Fig. 2a**, black circles) and standard deviation of peak ITDs as a function of neuronal BF indicate that neurons with the lowest BFs tended to have the highest values of peak ITD, whereas neurons with the highest BFs tended to have the lowest values of peak ITD. The few neurons with best delays at negative ITDs (**Fig. 2a**, white circles, absolute peak ITD) showed a similar relationship between BF and ITD. The dotted horizontal line indicates the maximum ITD experienced by the guinea pig (approximately  $\pm 150$   $\mu$ s). Plotted as the equivalent interaural phase disparities (IPDs; **Fig. 2b**), peak IPD tuning was independent of BF. This does not mean that individual neurons showed frequency-dependent ITD tuning. The central tenet of the Jeffress model of coincidence detection is that individual low-frequency binaural neurons show a unique or characteristic delay at which they respond maximally, independent of stimulating frequency. As we have reported previously<sup>32</sup>, IC neurons that respond in a manner consistent with this model also show the same dependence of peak (or characteristic) delay on neuronal

varied systematically along the main frequency axis. Maximum output of the lowest BF neurons occurred at long interaural delays, and maximum output of the highest BF neurons occurred at short interaural delays. The consequence of this arrangement was that the steepest slopes of ITD functions were positioned near midline ITDs, irrespective of neuronal BF. Furthermore, the rate at which neural output changed with interaural delay was a constant proportion of total neural output per microsecond of ITD, independent of BF.

Our data, consistent with suggestions made by previous authors<sup>23,24</sup>, indicate that for mammalian localization, the position of the peaks of ITD functions may be unimportant compared with the position of greatest sensitivity to the change in ITD. Our data support a model of low-frequency localization based on broadly tuned channels in the two sides of the brain<sup>25–27</sup>.

## RESULTS

### Peak ITD varies systematically with BF

We recorded responses of 520 low-BF neurons (< 2.0 kHz) from the left inferior colliculus (IC) of anesthetized guinea pigs to interaurally delayed broad-band noise, and examined their sensitivity to ITDs as a function of neuronal BF. Noise-delay functions (NDFs) were recorded from IC neurons with BFs (**Fig. 1a**) ranging from 250 Hz to 1.4 kHz, covering the frequency range over which ITD sensitivity is found in mammals. Whether for indi-



**Fig. 2.** Peak ITD, but not peak IPD, depends on neuronal BF. (a) Distribution of peak ITDs as a function of neuronal BF, for 100-Hz bands covering the full frequency range over which mammals are sensitive to interaural time differences in the stimulus fine structure. Error bars show standard deviations. Black circles show mean values for neurons with positive peak ITDs. White circles show absolute mean values for neurons with negative peak ITDs. Due to the small number of neurons with negative peak ITDs, neurons were divided into just 4 groups: BFs up to 200 Hz ( $n = 5$ ), BFs between 200 Hz and 400 Hz ( $n = 5$ ), BFs between 400 Hz and 600 Hz ( $n = 9$ ) and BFs above 600 Hz ( $n = 12$ ). Inset replots the standard deviations of those neurons with positive peak ITDs as a function of BF. (b) Same data as in (a), but plotted in terms of interaural phase disparity, where the best interaural phase (BP) was calculated as  $BP = \text{peak ITD (ms)} \times \text{BF (kHz)}$ . The inset replots the standard deviations as a function of BF for the IPD data.

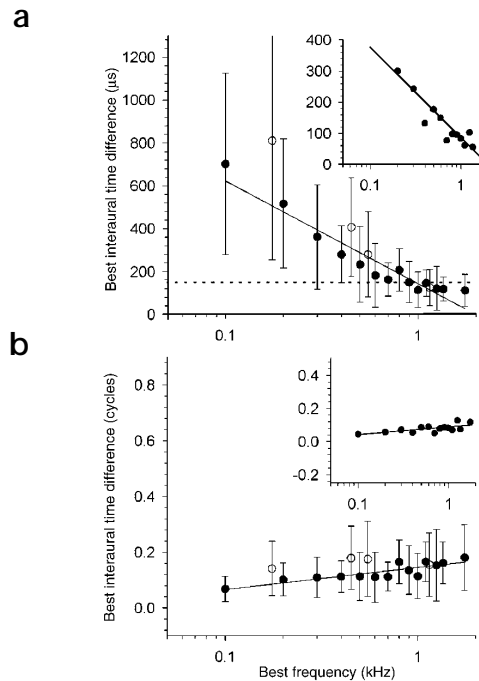
BF as we report here. In addition, those IC neurons that deviate from simple 'Jeffress-type' behavior show evidence of convergent binaural inputs from brainstem neurons with characteristic delays that seem to demonstrate the same relationship between BF and characteristic delay<sup>33</sup>.

A second feature of our data is that the range of ITDs encoded within each frequency channel also varied with BF. This is obvious from the standard deviations of the mean values, but is seen more clearly when the standard deviations are plotted against BF (Fig. 2a, inset). The peaks of the low-BF neurons occurred over a wide, non-physiological range of ITDs, whereas the peaks of high-BF neurons occurred over a restricted but more physiological range of ITDs. Standard deviations represented in terms of IPD, however, were largely independent of BF. This variation with BF of the mean and the range of peak ITDs is inconsistent with many current models of mammalian low-frequency binaural localization. Such models assume the full range of internal delay lines within each frequency channel distributed across the physically realizable range of ITDs<sup>10</sup>.

In Fig. 1a and b, the abscissa ranges have been adjusted to show the NDF shape in full, and indicate that NDFs are similar in shape across different BFs. However, when plotted over a smaller range of ITDs (Fig. 3a), the differences in scaling become apparent. As we demonstrated above for noise stimulation, and as we have reported previously for tones<sup>32</sup>, the ITD corresponding to the peak of the delay functions varied systematically with BF. However, a second, obvious feature from Fig. 3a is that NDFs for neurons with the lowest BFs were relatively broad compared to those for neurons with the highest BFs. This is because NDFs are quasi-periodic<sup>34</sup>, with the width of their main peak determined largely by the period of the BF component of the noise stimulus<sup>5,34,35</sup>. Consequently, for neurons with the lowest BFs, variation of the ITD by up to several hundred microseconds around the peaks of both individual and averaged NDFs had relatively little effect on the discharge rate. In contrast, small changes in ITD within the physiological range (dotted vertical lines) produced a relatively large change in discharge rate.

#### Delay functions are steepest around midline ITDs

For each of the 432 neurons with peaks at contralateral ITDs, a steepness function was obtained by calculating the absolute value of the slope of the function at each ITD. Two main features were observed for both individual NDFs (Fig. 1b, red curve in top panel) and averaged NDFs (Fig. 1b, red curves in remaining panels). First, NDFs tended to be steeper on the slope of the function on the midline side (that is, facing zero ITD) than on the slope of the function on the side away from midline. Eighty per-

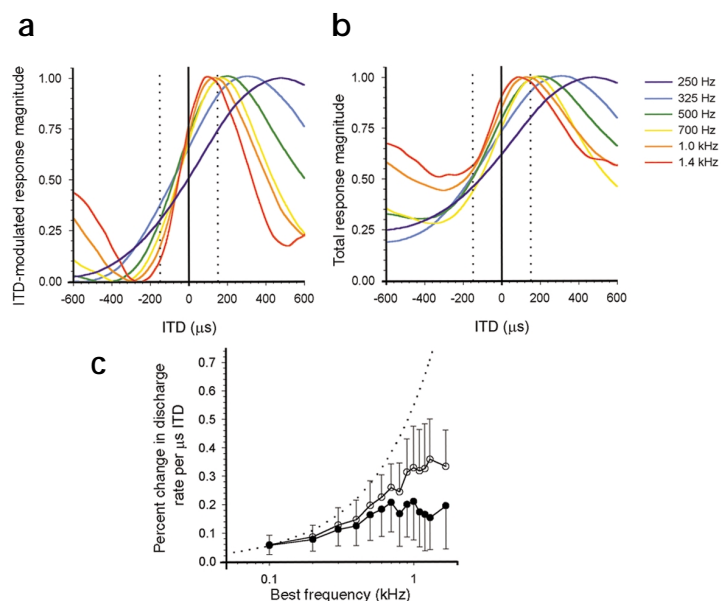


cent (346/432) of neurons with NDF peaks at positive ITDs showed steeper midline than non-midline sides of their NDFs, compared with just 11% (49/432) that showed steeper non-midline than midline sides, and 9% (37/432) that showed similarly steep midline and non-midline facing sides. Second, the steepest portion of the NDFs occurred close to zero ITD, and certainly within the physiological range of the guinea pig. Across all BFs, the distribution of ITDs at which NDF were steepest (Fig. 1d, red bars) indicated that many NDFs were steepest within the physiological range of the guinea pig (indicated by vertical dotted lines), and close to zero ITD.

**A rate code for interaural delay independent of neural BF**  
Responses of low-BF (< 1.0 kHz) MSO cells are highly modulated with ITD and generally show half-wave-rectified ITD functions, with the lowest BF neurons (< 200 Hz) showing even better than half-wave-rectified ITD functions<sup>29</sup>. This accords with the bushy cells in the ventral cochlear nucleus, the presumed inputs to the MSO coincidence detectors, enhancing monaural phase locking over that seen in primary auditory nerve fibers at these low frequencies<sup>36</sup>. In addition, there is a tendency for modulation to be reduced with increasing BF, presumably reflecting the reduction in phase locking of the presumed monaural inputs that is observed with increasing frequency<sup>36</sup>. We observed similar behavior in the responses of IC neurons. However, despite the tendency for ITD tuning systematically to become broader than half-rectified with increasing BF, the slopes of NDFs remained steeper for high- than for low-BF neurons (Fig. 3a). From this, one might conclude that the rate at which discharge rate changes when ITD is varied is a further metric that depends on neuronal BF. However, an important consideration is that the NDFs in Fig. 3a constitute functions that have been normalized for both the minimum and maximum evoked spike rates, and thus correspond to the ITD-modulated component only of the response to interaurally delayed noise. Analyzing the data in this format is consistent with previous



**Fig. 3.** The rate at which discharge rate changes as a function of ITD is largely independent of neuronal BF. **(a, b)** Average NDFs, plotted over the same ITD range, for neurons with BFs in bands around 250 Hz, 335 Hz and 425 Hz (both 50-Hz bands), 500 Hz, 700 Hz, 1.0 kHz and 1.4 kHz. The widest NDF with the longest peak ITD is that for the 250-Hz band (dark blue line). The BF band increases monotonically with decreasing NDF width and position of peak ITD up to 1.4 kHz (indicated by systematic transformation from 'cool' (blue) to 'hot' (red) colors as the peaks shift toward zero ITD). In **(a)**, the NDFs have been normalized for both the maximum and the minimum evoked discharge rates, that is, to show the ITD-modulated component only of the response at each BF. In **(b)**, the NDFs have been normalized for discharge rate maximum only, and show both the ITD-modulated and ITD-insensitive components of the response at each BF. **(c)** The rate of change of discharge rate per microsecond of ITD at 0  $\mu$ s examined in 100-Hz BF bands from 100 Hz to 1.4 kHz with a final band covering BFs up to 2 kHz. Dotted line indicates the percentage change in discharge rate per microsecond expected if neurons showed half-rectified NDFs. White circles indicate percentage change in discharge rate per microsecond calculated from the ITD-modulated components of the response only **(a)**. Black circles indicate the percentage change in discharge rate per microsecond calculated from the total discharge rate **(b)**.



studies of ITD processing<sup>31,37</sup>. However, the potential relevance to the responses of low-frequency IC neurons of input from monaural and ITD-insensitive nuclei is ignored in this analysis. When NDFs were normalized for maximum discharge rate only (**Fig. 3b**), rather than for both maximum and minimum discharge rate (**Fig. 3a**), the ITD-modulated component of the response as a proportion of the total neural output systematically declined with BF. The consequence of this increase in the magnitude of the non ITD-modulated response component is that the slopes of NDFs were more similar across BF than would be the case if neural output were modulated completely with ITD. As suggested by the NDFs in **Fig. 3a**, when only the ITD-modulated component of the responses were considered (**Fig. 3c**, white circles), the rate at which discharge rate changed with changing ITD increased systematically with increasing BF, albeit more slowly than predicted from the assumption of half-rectified responses (**Fig. 3c**, dotted line). When normalized to maximum spike output only (**Fig. 3c**, black circles), and therefore expressed as a proportion of total neural output (as with NDFs in **Fig. 3b**), the rate at which discharge rate changed with ITD was virtually constant across BFs. For the lowest BF neurons (centered at 100 Hz), NDFs essentially took the form of a half-rectified sine wave at BF being almost fully modulated with ITD. With increasing BF, however, the rate of change in discharge rate increased only slowly up to 400 Hz, and then remained essentially constant between 0.1% and 0.2% of discharge rate per microsecond ITD for BFs above 400 Hz.

#### DISCUSSION

The current explanation of low-frequency localization in mammals is that an array of neurons, tuned to different ITDs, encodes the position of a sound source in azimuth. The assumption implicit in this explanation is that tuning to a specific ITD is manifested as a maximum firing rate to that ITD, and that a range of neurons with peak firing rates covering the entire range of physiological ITDs exists within each auditory frequency band. Here we have

presented empirical evidence, based on the responses of a large population of ITD-sensitive single neurons, that is not consistent with this explanation. First, the representation of interaural delays across the physiological range by peak firing rates was not complete across the low-frequency tonotopic gradient. Rather, the position of peak ITDs was BF dependent, with the consequence that neurons showed the largest changes in their discharge rate with changes in ITD within the physiological range, and particularly for ITDs that correspond to midline spatial positions. Second, the extent of the representation within each frequency band was not equivalent across BF, with a much wider range of ITDs producing maximum firing in lower-BF than in higher-BF neurons. However, both the value and the range of the interaural phase difference at the peak within each frequency band were essentially invariant as a function of BF. These observations do not accord with current models of low-frequency binaural processing.

Anatomical evidence suggests that the barn owl nucleus laminaris (NL, the avian homologue of the mammalian MSO) contains a full complement of delay lines within each frequency channel<sup>18</sup>. Azimuthal position of a sound source is thought to be encoded by a population of neurons sharply tuned for ITDs within the barn owls' physiological range. This model of sound localization is normally taken *de facto* as the model to explain sensitivity to ITDs in mammals<sup>10</sup>, particularly as it accords extremely well with the coincidence detection model first proposed by Jeffress for human low-frequency sound localization<sup>3</sup>. However, aside from the empirical evidence in the current study, there are *a priori* reasons why a neural code in which the maximum discharge rate signals the ITD might not be sufficient to explain mammalian sensitivity to ITDs. Barn owls, using high frequencies with consequent narrow ITD tuning and many peaks of ITD functions within the physiological range<sup>12,15,17</sup>, would seem to have sufficient resolution in ITD functions to be able to use the peak firing rate. However, the broad ITD functions, and the lack of peaks near zero ITD, represent a problem for mammals working at much lower frequencies. In our data,



ITD tuning in the IC was only as sharp as that reported in the one study in which recordings were unequivocally confined to within the boundaries of the MSO<sup>29</sup>. Nevertheless, it remained that the slopes of ITD functions were sharper on the midline side of the peak ITD compared with the non-midline side. How might this observation, which has been previously reported<sup>38</sup>, be explained without resorting to a specific mechanism of neural sharpening? On the basis that there are long delays at low BFs and short delays at high BFs, convergent input onto single IC neurons from MSO neurons with different BFs, which is a linear additive process<sup>33,39</sup>, will produce NDFs with steeper midline than non-midline slopes as a matter of course. This is because individual NDFs are similar near midline but less so farther from it (Fig. 3a and b). The simplest explanation, therefore, for the difference in the steepness of the slopes of NDFs facing toward or away from midline ITDs, is that convergent excitatory input from the brainstem reduces the slope of functions away from midline, rather than inhibitory inputs sharpening the slope nearest the midline.

Plausible mechanisms that dispense entirely with axonal conduction delays have been postulated to account for the empirical observation of ITD sensitivity<sup>40</sup>. However, the current data remain consistent with the more established models of low-frequency binaural interactions including the involvement of MSO neurons as coincidence detectors. One question the current study raises concerns the nature and extent of any putative systematic arrangement of delay lines subserving ITD sensitivity. The extensive data set we report here clearly demonstrates that there is a strong relationship between BF and peak ITD in the mammalian midbrain. Because the MSO is tonotopically organized, there must be a topographical organization of differences in transmission time from the two ears that follows the tonotopy. However, we cannot rule out some additional form of processing that modifies either the input or the output of the MSO so that it reflects the pattern of responses we observe in the IC.

More important is the question of how the relationship between BF and peak ITD can contribute to mammalian sound localization. As an alternative model to a labeled line code, where a particular neuron firing maximally indicates the azimuthal position of the source, our data suggest that azimuth could be encoded in the form of a rate code mediated by broadly tuned spatial channels. The specific form this model might take is subject to debate<sup>26,27</sup>. At least three possibilities exist. The first is that azimuthal position of a sound source is computed from the overall discharge rate within the broadly tuned ITD channel on one side of the brain. Thus, for a sound moving away from the midline, activity will increase in the contralateral hemisphere, toward the peak of the ITD functions, indicating that the sound source has shifted to a more lateral position. An inherent ambiguity in this model arises, however, because changes in stimulus level also alter the overall activity within these broad channels. This potential ambiguity can be resolved by computing azimuthal position from a comparison of activity between hemispheric channels, corresponding to the summed (or subtracted) activity on either side of the brain<sup>25–27</sup>, or from comparison between binaural and monaural activity within the same hemispheric channel. In the two-hemispheric-channel model, an increase in activity because of a change in azimuthal position in one channel is accompanied by a decrease in activity in the other hemispheric channel. Because the low-pass filter properties of the head provide no appreciable interaural level differences for low-frequency sounds, irre-

spective of their position in space, changes in azimuth will have negligible effect on the sound-level-mediated component of the discharge rate. Thus, in the single-hemispheric model, changes in binaurally evoked, ITD-dependent activity are compared with a fixed and azimuth-independent level of monaural activity in the same side of the brain. One potential problem for a localization model based on the comparison of activity in two hemispheric binaural channels is that unilateral lesions of the IC seem to produce only contralateral deficits in sound localization<sup>41</sup>. However, because this study used broad-band stimulation that would produce ITD, ILD and spectral cues, it is possible that a binaural deficit in ITD processing alone could be masked by the use of the other cues.

The provision for exquisite sensitivity to ITDs by the use of broadly tuned channels is consistent with processing in many other sensory modalities and submodalities, including color processing in the visual system, in which cells broadly tuned for wavelength provide for sensitivity to a plethora of different hues. Furthermore, the representation of broadly tuned, low-frequency spatial channels within each hemisphere is similar to the activity patterns generated at high frequencies by interaural level differences. Although a small fraction of mammalian neurons sensitive to disparities in the level of a sound at the two ears are selectively tuned to a specific ILD, most favor activation of one ear over the other, with maximal modulation of discharge rates for ILDs corresponding to midline, or near-midline, spatial positions<sup>42,43</sup>. This again contrasts with the barn owl, for which the ILD-sensitive neurons in the IC are sharply tuned to a specific elevation which, when combined with the output of neurons sharply tuned for azimuth, provides for a space-specific map in the barn owl optic tectum<sup>17</sup>. Empirical evidence suggests that the azimuth of high-frequency sound sources may be encoded primarily by edges in azimuth receptive fields of a population of ILD-sensitive cells<sup>43</sup>. This is consistent with the suggestion that the slopes of the functions through midline provide the basis for spatial acuity even when spectral localization cues arising from the outer ear are included.

## METHODS

Single-neuron recordings were made from the low-frequency regions of the inferior colliculus of 133 urethane-anesthetized guinea pigs using glass-coated tungsten microelectrodes. Data from these animals contributed to a range of different studies investigating binaural hearing over a three-year period, as well as to the experiments reported here. All experiments were carried out in accordance with the Animal (Scientific Procedures) Act of 1986 of Great Britain and Northern Ireland. Following isolation, each neuron's BF was first determined audio-visually using binaurally presented tones presented at zero ITD, and then by recording a detailed frequency-versus-level response area over a 6-octave range around this BF. Ninety-five percent of the neurons sampled had BFs below 1.5 kHz, a frequency close to the upper limit of ITD sensitivity in the guinea pig<sup>32</sup>. Noise stimuli consisted of identical (frozen) broadband noise bursts (50 Hz–5 kHz) presented dichotically to each ear using 12.7-mm Brüel and Kjaer (Nærum) condenser earphones at 10–20 dB above the neuron's noise threshold. Noise-delay functions (NDFs) were constructed over a range of interaural delays equal to 3× the period of the neuron's BF. Either 20 repetitions of a 50-ms burst of noise, or 3 repetitions of a 320-ms burst of noise were presented at each of 51 equally spaced delays over this range. Steepness functions were constructed for each NDF by calculating the absolute slope for each ITD from the difference in spike counts evoked by the two neighboring ITDs, one more negative and one more positive. Further details of methods may be found in our previous reports of ITD-sensitive responses to interaurally delayed noise<sup>44</sup>.



RECEIVED 10 OCTOBER 2000; ACCEPTED 27 FEBRUARY 2001

1. Rayleigh, Lord On our perception of sound direction. *Philos. Mag.* **13**, 214–232 (1907).
2. Stevens, S. S. & Newman, E. B. The localization of actual sources of sound. *Am. J. Psychol.* **48**, 297–306 (1936).
3. Jeffress, L. A. A place theory of sound localization. *J. Comp. Physiol. Psychol.* **41**, 35–39 (1948).
4. Wightman, F. L. & Kistler, D. J. The dominant role of low-frequency interaural time differences in sound localisation. *J. Acoust. Soc. Am.* **85**, 868–878 (1992).
5. Yin, T. C. T. & Kuwada, S. Binaural interaction in low-frequency neurons in inferior colliculus of the cat. III. Effects of changing frequency. *J. Neurophysiol.* **50**, 1020–1042 (1983).
6. Kuwada, S., Stanford, T. R. & Batra, R. Interaural phase-sensitive units in the inferior colliculus of the unanesthetized rabbit: effects of changing frequency. *J. Neurophysiol.* **57**, 1338–1360 (1987).
7. Palmer, A. R., Rees, A. & Caird, D. in *Processing of Complex Sounds by the Auditory System* (eds. Carlyon, R. P., Darwin, C. J. & Russell, I. J.) 415–422 (Clarendon, Oxford, 1992).
8. Spitzer, M. W. & Semple, M. N. Transformation of binaural response properties in the ascending auditory pathway: influence of time-varying interaural phase disparity. *J. Neurophysiol.* **80**, 3062–3076 (1998).
9. Takahashi, T. & Konishi, M. Selectivity for interaural time difference in the owl's midbrain. *J. Neurosci.* **6**, 3413–3422 (1986).
10. Stern, R. M. & Trahiotis, C. in *Binaural and Spatial Hearing in Real and Virtual Environments* (eds. Gilkey, R. H. & Anderson, T. R.) 499–531 (Erlbaum, Mahwah, New Jersey, 1996).
11. Coles, R. B. & Guppy, A. Directional hearing in the barn owl (*Tyto alba*). *J. Comp. Physiol. A* **163**, 117–133 (1988).
12. Wagner, H., Takahashi, T. & Konishi, M. Representation of interaural time differences in the central nucleus of the barn-owl's inferior colliculus. *J. Neurosci.* **7**, 3105–3116 (1987).
13. Zwislocki, J. & Feldman, R. S. Just noticeable differences in dichotic phase. *J. Acoust. Soc. Am.* **28**, 866–864 (1956).
14. Middlebrooks, J. C. & Green, D. M. Sound localisation by human listeners. *Annu. Rev. Psychol.* **42**, 135–159 (1991).
15. Knudsen, E. I. & Konishi, M. Mechanisms of sound localisation in the barn owl (*Tyto alba*). *J. Comp. Physiol.* **133**, 13–21 (1979).
16. Takahashi, T., Moiseff, A. & Konishi, M. Time and intensity cues are processed independently in the auditory system of the owl. *J. Neurosci.* **4**, 1781–1786 (1984).
17. Olsen, J. F., Knudsen, E. I. & Esterly, S. D. Neural maps of interaural time and intensity differences in the optic tectum of the barn-owl. *J. Neurosci.* **9**, 2591–2605 (1989).
18. Carr, C. E. & Konishi, M. A circuit for detection of interaural time differences in the brainstem of the barn owl. *J. Neurosci.* **10**, 3227–3246 (1990).
19. Smith, P. H., Joris, P. X. & Yin, T. C. T. Projections of physiologically characterized spherical bushy cell axons from the cochlear nucleus of the cat: evidence for delay lines in the medial superior olive. *J. Comp. Neurol.* **331**, 245–260 (1992).
20. Beckius, G. E., Batra, R. & Oliver, D. L. Axon from anteroventral cochlear nucleus that terminates in medial superior olive of the cat: observations related to delay lines. *J. Neurosci.* **19**, 3146–3161 (2000).
21. Domintz, R. H. & Colburn, H. S. Lateral position and interaural discrimination. *J. Acoust. Soc. Am.* **61**, 1586–1598 (1977).
22. Curcio, C. A., Sloan, K. R., Packer, O., Hendrickson, A. E. & Kalina, R. E. Distribution of cones in human and monkey retina: individual variability and radial asymmetry. *Science* **236**, 579–582 (1987).
23. Stillman, R. D. Characteristic delay neurons in the inferior colliculus of the kangaroo rat. *Exp. Neurol.* **32**, 404–412 (1971).
24. Phillips, D. P. & Brugge, J. F. Progress in neurophysiology of sound localisation. *Annu. Rev. Psychol.* **36**, 245–274 (1985).
25. von Békésy, G. Zur theorie des hörens. Über das richtungshören bei einer zeitdifferenz oder lautstärkenungleichheit der beiderseitigen schalleinwirkungen. *Physik. Z.* **31**, 824–835 (1930).
26. van Bergeijk, W. A. Variation on a theme of von Békésy: a model of binaural interaction. *J. Acoust. Soc. Am.* **34**, 1431–1437 (1962).
27. Colburn, H. S. & Latimer, J. S. Theory of binaural interaction based on auditory-nerve data III. Joint dependence on interaural time and amplitude differences in discrimination and detection. *J. Acoust. Soc. Am.* **64**, 95–106 (1978).
28. Elverland, H. H. Ascending and intrinsic projections of the superior olivary complex in the cat. *Exp. Brain Res.* **32**, 117–134 (1978).
29. Yin, T. C. T. & Chan, J. C. K. Interaural time sensitivity in medial superior olive of cat. *J. Neurophysiol.* **64**, 465–488 (1990).
30. Spitzer, M. W. & Semple, M. N. Neurons sensitive to interaural phase disparity in gerbil superior olive: diverse monaural and temporal response properties. *J. Neurophysiol.* **73**, 1668–1690 (1995).
31. Batra, R., Kuwada, S. & Fitzpatrick, D. C. Sensitivity to interaural temporal disparities of low- and high-frequency neurons in the superior olivary complex. I. Heterogeneity of responses. *J. Neurophysiol.* **78**, 1222–1236 (1997).
32. McAlpine, D., Jiang, D. & Palmer, A. R. Interaural delay sensitivity and the classification of low best-frequency binaural responses in the inferior colliculus of the guinea pig. *Hear. Res.* **97**, 136–152 (1996).
33. McAlpine, D., Jiang, D., Shackleton, T. M. & Palmer, A. R. Convergent input from brainstem coincidence detectors onto delay-sensitive neurons in the inferior colliculus. *J. Neurosci.* **18**, 6026–6039 (1998).
34. Yin, T. C. T., Chan, J. C. K. & Irvine, D. R. F. Effects of interaural time delays of noise stimuli on low-frequency cells in the cat's inferior colliculus. I. Responses to wideband noise. *J. Neurophysiol.* **55**, 280–300 (1986).
35. Yin, T. C. T., Chan, J. C. K. & Carney, L. H. Effects of interaural time delays of noise stimuli on low-frequency cells in the cat's inferior colliculus. III. Evidence for cross-correlation. *J. Neurophysiol.* **58**, 562–583 (1987).
36. Joris, P. X., Carney, L. H., Smith, P. H. & Yin, T. C. T. Enhancement of neural synchronization in the anteroventral cochlear nucleus. I. Responses to tones at the characteristic frequency. *J. Neurophysiol.* **71**, 1022–1036 (1994).
37. Fitzpatrick, D. C., Batra, R., Stanford, T. R. & Kuwada, S. A neuronal population code for sound localisation. *Nature* **388**, 871–874 (1997).
38. Kuwada, S., Batra, R. & Fitzpatrick, D. C. in *Binaural and Spatial Hearing in Real and Virtual Environments* (eds. Gilkey, R. H. & Anderson, T. R.) 399–426 (Erlbaum, Mahwah, New Jersey, 1997).
39. Shackleton, T. M., McAlpine, D. & Palmer, A. R. Modelling convergent input onto interaural-delay-sensitive inferior colliculus neurons. *Hear. Res.* **149**, 199–215 (2000).
40. Shamma, S. A., Shen, N. & Gopalaswamy, P. Stereausis: binaural processing without neural delays. *J. Acoust. Soc. Am.* **86**, 989–1006 (1989).
41. Jenkins, W. M. & Masterton, R. B. Sound localization: effects of unilateral lesions in central auditory system. *J. Neurophysiol.* **47**, 987–1016 (1982).
42. Wenstrup, J. J., Ross, L. S. & Pollak, G. D. Binaural response organization within a frequency-band representation of the inferior colliculus: implications for sound localization. *J. Neurosci.* **6**, 964–973 (1986).
43. Delgutte, B., Joris, P. X., Litovsky, R. Y. & Yin, T. C. T. Receptive fields and binaural interactions for virtual space stimuli in the cat inferior colliculus. *J. Neurophysiol.* **81**, 2833–2851 (1999).
44. Jiang, D., McAlpine, D. & Palmer, A. R. Detectability index measures of binaural masking level differences across populations of inferior colliculus neurons. *J. Neurosci.* **17**, 9331–9339 (1997).